

Phase transitions in $\text{La}_{1-x}\text{Ca}_x\text{MnO}_3$

I. O. Troyanchuk

Institute of Solid State Physics and Semiconductors, Academy of Sciences of Belorussia

(Submitted 10 January 1992)

Zh. Eksp. Teor. Fiz. **102**, 251–261 (July 1992)

The crystal structure of thermal expansion and the elastic properties of manganites with perovskite structure were investigated. It is shown that antiferrodistortional ordering of d_{z^2} orbitals occurs in AMnO_3 (A—La, Pr, Nd, Tb). The transition into the orbitally disordered phase is a first-order transition with a large temperature interval of coexistence of the phases and with temperature hysteresis. The crystal-structural phases diagram of $\text{La}_{1-x}\text{Ca}_x\text{MnO}_3$ is constructed. The dynamic and static magnetic properties of $\text{La}_{1-x}\text{Ca}_x\text{MnO}_3$ were investigated. The magnetic phase diagram was constructed. The experimental facts indicate that the antiferromagnet–ferromagnet concentration transition occurs through a mixed two-phase state. The magnetic transformations result from transformations of the crystal structure. The regions in the T - x plane where the conductivity decreases with increasing temperature, as happens in metals, were determined from investigations of the electric properties. Mechanisms are proposed for the transitions. Arguments are presented in support of the fact that the magnetic properties are governed by superexchange via anions and not exchange interactions via carriers, as is suggested in a number of works.

1. INTRODUCTION

Antiferromagnet–ferromagnet and insulator–metal transitions have been observed in the orthomanganites $\text{La}_{1-x}\text{Ca}_x(\text{Mn}^{3+}\text{Mn}^{4+})\text{O}_3$ ($\text{C-Ca}^{2+}\text{Pb}^{2+}\text{Ba}^{2+}$) for $x \geq 0.2$ with perovskite structure.¹ It was observed that as the temperature increases the ferromagnet–paramagnet transition is accompanied by a transition from metallic to activated conductivity.² In Ref. 3 it is shown that the transition temperatures may be different. In order to explain the reasons for the transitions Zener introduced a special form of the exchange interactions via carriers—double exchange.⁴ De Gennes⁵ developed the theory of double exchange and predicted that a noncollinear magnetic structure forms at intermediate concentrations between the antiferromagnetic and ferromagnetic states. The neutron diffraction data^{6,7} can be interpreted both as realization of a noncollinear magnetic structure and assuming a mixed two-phase state. Measurements in strong magnetic fields were interpreted in favor of the existence of a noncollinear magnetic structure.⁸ In Ref. 9 it is suggested that ferrons are formed in the intermediate region. In the last few years there have appeared articles in which the properties of orthomanganites are explained on the basis of the RKKY theory.³ In Refs. 10 and 11, however, doubts were cast on the existence of strong exchange interaction via charge carriers.

Goodenough¹² has suggested that ferromagnetism is governed not only by strong double exchange but also by the specific nature of the exchange interactions in the system of Jahn–Teller ions Mn^{3+} . He proposed that the orbital configuration of the $3d$ electrons in the case when the static Jahn–Teller distortions are removed is determined by the position of the nuclei of the ions (Goodenough's quasistatic hypothesis). In this case dynamic enhancement of the ferromagnetic part of the exchange interactions occurs. In Ref. 13 it was observed that the magnetic properties are correlated with the unit-cell parameters. Havinga presents arguments in favor of the fact that the sign of the exchange interactions is determined by the magnitude of the Mn–O–Mn angle.¹⁴

There is no general agreement concerning the changes

brought about in the crystal structure as a result of orbital ordering. Goodenough proposed that the ground state is d_{z^2} , while in Refs. 15 and 16 it is asserted that the ground state is $d_{x^2-y^2}$. X-ray crystallographic studies of LaMnO_3 indicate that the removal of the static Jahn–Teller distortions is a first-order phase transition, while dilatometric investigations did not show any jump in the length of the sample.¹⁵

In the present work a comprehensive investigation was made of the crystal structure and the magnetic and electric properties of orthomanganites in order to explain the reasons for the phase transformations. The data obtained by different methods of measurement of the properties and synthesis of the samples are analyzed.

2. EXPERIMENTAL PROCEDURE

The method of preparation and the crystal-structural characteristics of the $\text{La}_{1-x}\text{Ca}_x\text{MnO}_3$ samples, which are stoichiometric with respect to oxygen, are described in Ref. 17. The conditions of synthesis and the parameters of the crystal structure of nonstoichiometric samples $\text{La}_{1-x}\text{Ca}_x\text{Mn}^{3+}\text{O}_{3-x/2}$ are presented in Ref. 18. Samples of RMnO_3 (R ranges from Pr to Dy) were prepared by quenching in air. In the cases R —Y, Ho, Tm, and Yb synthesis was conducted under high pressure. The unit-cell parameters of this series of samples were identical to the values obtained in Refs. 16 and 18.

X-ray structural analysis was performed on a DRON-3 diffractometer in Fe K_α radiation in the temperature interval from 100 to 1300 K. The O' and O orthorhombic phases were separated by the method described in Ref. 15. Young's modulus was measured by the resonance method on cylindrical samples 70 mm long and 7 mm in diameter at temperatures 110–600 K. A mechanical dilatometer was employed to measure the thermal expansion. Samples at least 30 mm long were employed to reduce the measurement error.

The dynamic magnetic susceptibility was measured with a mutual inductance/bridge. The amplitude of the field was equal to 200 A/m and the frequency was equal to 1000 Hz. The magnetization was measured with a vibration mag-

netometer. The relative error of measurement did not exceed 2%.

The electric conductivity was measured by the four-contact method. Indium-gallium eutectic or silver paste, which was fired on at 800 K, was employed for forming the contacts. The measurements were performed on well-sintered samples with a density of not less than 90% and with no macrocracks.

3. EXPERIMENTAL RESULTS AND DISCUSSION

3.1. Orbital ordering

In the literature there is no general agreement concerning orbital ordering in orthomanganites. To determine which orbital, d_{z^2} or $d_{x^2-y^2}$, is stabilized as a result of the Jahn–Teller effect, the Mn–O bond lengths in MnO_6 octahedra must be compared.¹² The coordinates of the ions in AMnO_3 ($A = \text{La, Pr, Nd, Tb}$) were determined in Ref. 18 by neutron-diffraction investigations. On the basis of the data obtained in Ref. 18 we calculated the distances between the ions in the MnO_6 octahedra (Table I). We found that in all compounds listed above two of the Mn–O bond lengths are significantly longer than the other four. This means that the d_{z^2} orbital is stabilized. In the case when the $d_{x^2-y^2}$ is stabilized, four of the Mn–O bond lengths should be longer than the other two, since the lobes of the $d_{x^2-y^2}$ orbitals are directed toward the four anions and the occupied orbital will repel them.

In Ref. 16 it was asserted, on the basis of analysis of the magnetic properties, that in YMnO_3 the $d_{x^2-y^2}$ orbital is stabilized. Unfortunately, there are no published data on the coordinates of ions in orthomanganates with heavy rare-earth ions (except A–Tb). We constructed the dependence of the unit-cell parameters of orthomanganates on the radius of the rare-earth ion Y . We found that as the radius of the A cation decreases the cell parameters decrease monotonically. In the case of a transition from ordering of d_{z^2} orbitals to ordering of $d_{x^2-y^2}$ orbitals it is difficult to explain this behavior.

Analysis of the distances between ions in different directions shows that in orthomanganates antiferrodistortional ordering of d_{z^2} orbitals is realized, as was first proposed by Goodenough,¹² on the basis of indirect data.

3.2. Removal of Jahn–Teller static distortions

According to the theory, in the case of antiferrodistortional ordering a phase transition into the orbitally disordered phase can be expected to occur as the temperature decreases.¹⁹ The transition must be of second order, but as noted in Ref. 19 the transition is of first order in the case of strong anisotropy.

Data on the transition into the orbitally disordered phase in LaMnO_3 are inconsistent.¹⁵ For this reason, we investigated the rare-earth manganites. The $\text{NdMnO}_{3.05}$ sam-

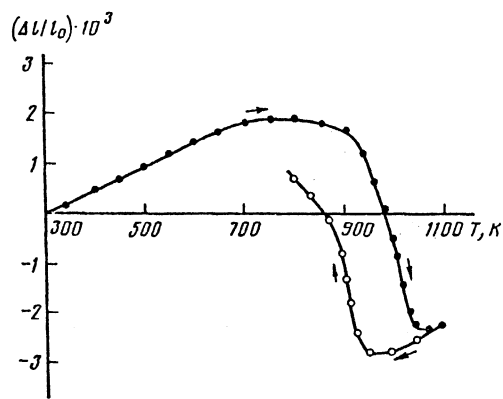


FIG. 1. Relative change in the length of a $\text{NdMnO}_{3.05}$ specimen as a function of the temperature.

ple is characterized by an O' orthorhombic unit cell. According to Goodenough, O' distortions are caused by orbital ordering. The unit-cell parameters a , b , and c are related as $c\sqrt{2} < a < b$ in the O' phase and $a < c\sqrt{2} < b$ in the O phase. Investigations of this sample by DTA and DTG methods in the temperature interval 300–1300 K did not reveal any sharp anomalies. However, dilatometric investigations showed that with increasing temperature the thermal expansion coefficient is negative in a significant temperature interval (Fig. 1). X-ray diffraction investigations in this temperature interval revealed that the O' and O phases coexist. As the temperature increases the O phase gradually displaces the O' phase. At a fixed temperature the relative content of both phases is independent of time; this is typical of martensite transformations. The transformation is accompanied by significant temperature hysteresis, reaching 100 K. The characteristic temperature at the end of the transformation is equal to 1150 K for NdMnO_3 , 1220 K for SmMnO_3 , and above 1300 K for GdMnO_3 . As the radius of the rare-earth ion decreases the transformation temperature increases. This probably happens because of an increase in the “seed” distortions of the MnO_6 octahedron as a result of the size effect.

In the case when the cooperative Jahn–Teller distortion of the lattice is removed, the following situations can be realized.

1. Static Jahn–Teller distortions of the octahedron remain, but there is no long-range order of the orbitals (Jahn–Teller glass).

2. Resonance coupling arises between $d_{x^2-y^2}$ and d_{z^2} states. Occupation of a definite state is determined by the vibrations of the anions. In this case dynamic correlation with occupation of states in the nearest octahedra is possible.

3. Resonance between the $d_{x^2-y^2}$ and d_{z^2} states exists, but the occupation of the orbitals is not correlated with the vibrations of the anions.

Infrared spectroscopy can yield definite information about the realization of these situations. This method is sensitive to short-range order. When the cooperative Jahn–Teller distortions are removed in the system $\text{La}_{1-x}\text{Ca}_x\text{MnO}_3$ in which the manganese ions have mixed valence, absorption of light by free carriers increases sharply, which makes it difficult to analyze the IR spectra. For this reason, this investigation was performed on the anion-deficient insulators $\text{La}_{1-x}\text{Ca}_x\text{MnO}_{3-x/2}$, in which the O' distortions are re-

TABLE I. Mn–O bond lengths in the orthomanganites AMnO_3 .

Compound	t , nm	m , nm	s , nm
LaMnO_3	0,2167	0,1959	0,1905
PrMnO_3	0,2172	0,1949	0,1922
NdMnO_3	0,2230	0,1931	0,1920
TbMnO_3	0,2251	0,1925	0,1890

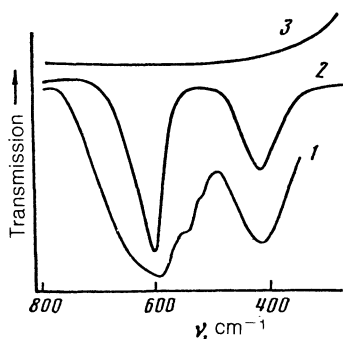


FIG. 2. IR absorption spectra of LaMnO_3 (1), $\text{La}_{0.6}\text{Ca}_{0.4}\text{MnO}_{2.8}$ (2), and $\text{La}_{0.7}\text{Ca}_{0.3}\text{MnO}_3$ (3).

moved for $x > 0.2$. The high-frequency absorption ($\nu \geq 500 \text{ cm}^{-1}$) is caused by vibrations within the MnO_6 octahedra.²⁰ In LaMnO_3 vibrational modes can be identified at the frequencies 510, 545, 590, and 630 cm^{-1} (Fig. 2). These modes correspond to vibrations of the Mn–O bonds. Vibrational modes below 500 cm^{-1} are more complicated: Mn–O as well as La–O vibrations participate in them. The peak at 440 cm^{-1} apparently consists of several unresolved vibrational modes. In nonstoichiometric manganite the width of the high-frequency modes decreased sharply (Fig. 2). It is natural to attribute the decrease in the width of the vibrational modes to the decrease in the magnitude of the distortions of the MnO_6 octahedra. LaMnO_3 is strongly O' -orthorhombically distorted, while nonstoichiometric manganite has very small O -orthorhombic distortions. We believe that the results of IR spectroscopy show that the electron transition frequency between different orbital states in nonstoichiometric manganite is higher than the optical-phonon frequency. In perovskite in which the manganese ions have mixed valence, the vibrational modes are screened by absorption by charge carriers.

3.3. Crystal-structural phase diagram

We constructed the crystal-structure phase diagram of the system $\text{La}_{1-x}\text{Ca}_x\text{MnO}_3$ (Fig. 3) on the basis of x-ray investigations of the crystal structure, elastic properties, and thermal expansion. The phase diagram of this system is very similar to the crystal structure phase diagram of the $\text{LaMnO}_{3+\lambda}$ system, first constructed in Ref. 15.

X-ray crystallographic analysis revealed with Ca concentrations up to $x = 0.15$ a wide interval in which the O' and O phases coexist. This is indicated by the fact that the (220) and (040) reflections from both phases are recorded simul-

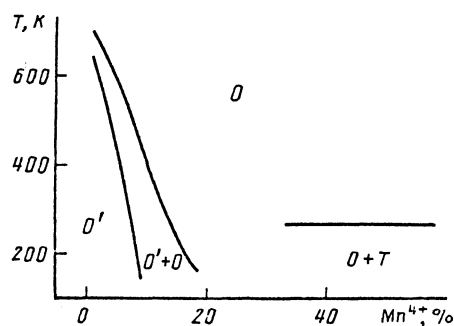


FIG. 3. Crystal-structure phase diagram of the system $\text{La}_{1-x}\text{Ca}_x\text{MnO}_3$.

taneously. Previous investigations of the system $\text{LaMnO}_{3+\lambda}$ yielded analogous results.¹⁵ In the region of coexistence of the phases the temperature dependence of Young's modulus is characterized by a strongly diffuse minimum. An anomaly appears on the dilatometric curves, and the thermal expansion coefficient becomes negative. A wide temperature interval of coexistence of phases is often observed with martensitic transformations, which occur with high activation energy in stress fields generated by different properties of both phases.

When the calcium ion concentration reaches $x = 0.4$ another crystal-structural transformation is observed somewhat below room temperature. This transformation is recorded according to the splitting of the (020) and (112) diffraction reflections and the appearance of a minimum in the temperature dependence of Young's modulus. The unit-cell parameters of the low-temperature phase are related as $c\sqrt{2} > a \approx b$, as against $c\sqrt{2} \approx a \approx b$ in the high-temperature phase. Such a transformation was investigated in detail previously in the system $\text{Pr}_{1-x}\text{Ca}_x\text{MnO}_3$.²¹ The temperature of this transformation is approximately the same in $x = 0.4$ and $x = 0.5$ samples. However the anomaly of Young's modulus in the $x = 0.5$ sample is more pronounced and less diffuse as a function of the temperature than in the case $x = 0.4$. In the $x = 0.4$ sample the profiles of some reflections become asymmetric as the temperature decreases below critical. For this reason, we assumed that in the $x = 0.4$ sample a nonuniform state consisting of domains of the quasitetragonal ($c\sqrt{2} \approx a < b$) and quasicubic ($c\sqrt{2} \approx a \approx b$) domains is realized at low temperatures. As in Ref. 21, we assume that the quasitetragonal phase results from ordering of heterovalent manganese ions and d_z^2 orbitals of the Mn^{3+} ions.

3.4. Magnetic properties

The $\text{La}_{1-x}\text{Ca}_x\text{MnO}_3$ samples can be grouped into four concentration intervals on the basis of their magnetic properties. Samples from the interval $x < 0.10$ are characterized by the presence of a single maximum in the temperature dependences of the imaginary $\chi''(T)$ and real $\chi'(T)$ parts of the differential magnetic susceptibility. In the case of heating in weak magnetic fields, a maximum is observed in the temperature dependences $\sigma(T)$ (Fig. 4); after cooling in a field this maximum is not present (Fig. 5). Magnetization saturation was not observed in fields up to 1.6 mA/m. The

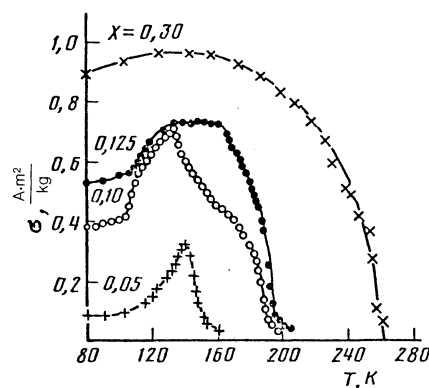


FIG. 4. Temperature dependence of the magnetization of $\text{La}_{1-x}\text{Ca}_x\text{MnO}_3$ in a field $H = 1.6 \cdot 10^3 \text{ A/m}$ after cooling in zero field ($H = 0$).

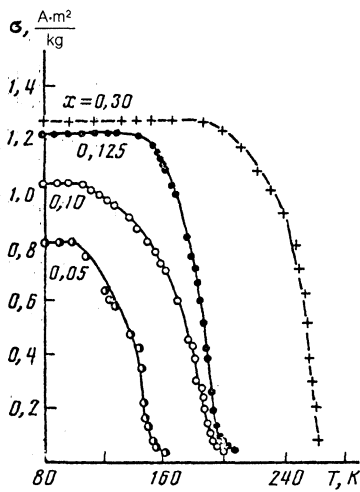


FIG. 5. $\sigma(T)$ for $\text{La}_{1-x}\text{Ca}_x\text{MnO}_3$. The temperature dependence was obtained in the field $H = 1.6 \cdot 10^3$ A/m after cooling in this field.

coercive force in LaMnO_3 at $T = 77$ K reaches a very high value of $2 \cdot 10^5$ A/m. After cooling in a magnetic field the hysteresis loop shifts relative to the origin of coordinates. As the calcium content increases the magnetization increases rapidly and the coercive force decreases. The residual magnetization relaxes logarithmically.

Two peaks in the $\chi''(T)$ curve and an anomaly at low temperatures in $\chi'(T)$ were observed for samples with $0.10 \leq x \leq 0.20$ (Fig. 6). The low-temperature anomaly is present in the $\sigma(T)$ curve in the heating regime and is absent after cooling in a field (Figs. 4 and 5). Increasing the magnetic field smoothes the anomaly. The field dependence of the magnetization is characterized by a strong para-process. The magnetic moment per formula unit is smaller than under conditions of ferromagnetic ordering of the magnetic moments of the manganese ions, but as the calcium content increases it gradually approaches the theoretical value for ferromagnetism. The following curious fact should be noted: The temperatures of the magnetic transformations change very little as the calcium content increases. In samples with $x = 0.15$ and $x = 0.175$ quite high residual magnetization was recorded right up to a temperature of 250 K; this could be due to inhomogeneity.

The magnetic properties in the interval $0.2 < x < 0.35$

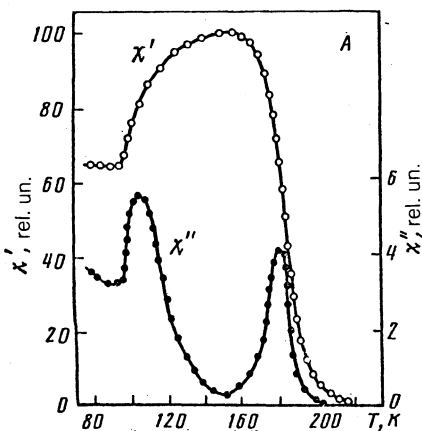


FIG. 6. Temperature dependence of χ' and χ'' for the sample $\text{La}_{0.875}\text{Ca}_{0.125}\text{MnO}_3$.

are typical for homogeneous ferromagnets. The magnetic moment reaches the value $3.3\mu_B$, which indicates ferromagnetism. Low-temperature anomalies were not observed in the temperature dependences $\chi(T)$ and $\sigma(T)$. The coercive force is small: about 10^4 A/m.

In samples with $x > 0.3$ the specific magnetization decreases sharply with increasing calcium content. A maximum appears in the curves $\chi(T)$ and $\sigma(T)$ in weak fields. The temperatures of the maxima are approximately the same in samples with $x = 0.4$ and $x = 0.5$. The residual magnetization remains significant up to a temperature close to T_c in samples belonging to the preceding interval.

3.5. Magnetic phase diagram

Figure 7 shows values of the critical temperatures of the magnetic phase transformations in the system $\text{La}_{1-x}\text{Ca}_x\text{MnO}_3$. We believe that samples in the interval up to $x < 0.10$ are antiferromagnets with inclusions of ferromagnetic clusters. This assumption is confirmed not only by the magnetic properties, but also by the neutron-diffraction data. According to Ref. 6, coherent magnetic scattering of neutrons is caused by antiferromagnetic A ordering.

Most investigators assume that in the interval $0.10 < x < 0.20$ the structure is uniform and noncollinear. We believe that in this interval a mixed state, consisting of antiferromagnetic and ferromagnetic phases, is realized. The neutron-diffraction data can be interpreted in several ways.^{6,7} However the first model contradicts the facts that the line of the low-temperature phase transformations in the region $0.1 < x < 0.2$ is a continuation of the line into the region $x < 0.1$ and that the samples exhibit properties characteristic of spin glasses. In the case of the transition noncollinear-collinear magnet the transformation temperature should depend sharply on the composition,⁵ and this was not observed.

Matsumoto²² observed, in an NMR investigation of magnetic phase transformations in $\text{La}_{1-x}\text{Ca}_x\text{MnO}_3$ with $x \geq 0.15$, signals from both separate Mn^{3+} and Mn^{4+} ions and from a phase with intermediate valence in which the Mn^{3+} and Mn^{4+} ions are indistinguishable because of rapid electronic exchange. The frequencies of the signals are virtually independent of the composition. According to our investigations, the transition into a new phase is accompanied by a jump of the Curie temperature. On the phase diagram the

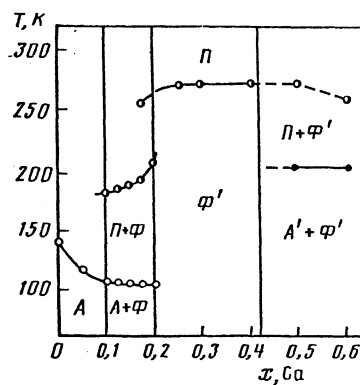


FIG. 7. Magnetic phase diagram of $\text{La}_{1-x}\text{Ca}_x\text{MnO}_3$: A —antiferromagnetic phase with A -type magnetic ordering; A' —phase with FE-type ordering; Φ —ferromagnetic dielectric phase; and, Φ' —phase with intermediate valence of manganese ions.

ferromagnetic dielectric phase is denoted as Φ while the ferromagnetic phase with intermediate valence of manganese ions is denoted as Φ' . The Φ' phase gradually displaces the Φ phase, and in the interval up to $x = 0.4$ the ferromagnetic phase with intermediate valence is mainly present.

In samples with $x > 0.4$ neutron-diffraction studies revealed an antiferromagnetic phase of the FE type.⁶ For the critical ordering temperature of this phase we adopted the maximum in the temperature dependence of the magnetic susceptibility. As in the case of preceding transformations, the A' phase gradually displaces the Φ' phase; this is typical of first-order phase transitions.

Phase stratification was observed in a number of oxide systems. In many cases phase stratification occurs at very low temperatures (even below room temperature, as in $\text{La}_2\text{CuO}_{4+\delta}$), when diffusion processes are very slow. For this reason, the phase-separation mechanism is controversial. In most cases, it is conjectured that separation occurs by the mechanism of spinodal decomposition of solid solutions. In the case of the system $\text{La}_{1-x}\text{Ca}_x\text{MnO}_3$ the parameters of the O' orthorhombic unit cell change significantly on substitution with Ca. The temperature of the $O'-O$ transition decreases. However the temperatures of the magnetic phase transformations in the corresponding phase are virtually independent of the concentration. It is possible that the $O'-O$ transition is not purely martensitic and is accompanied by definite diffusion processes, as a result of which the chemical composition of the magnetic phases remains constant.

3.6. Electric properties

For the system $\text{La}_{1-x}\text{Ca}_x\text{MnO}_3$ there are two regions in the T - x plane where the conductivity decreases with increasing temperature, as in the case of metals. We investigated the electric conductivity, and as a result of our investiga-

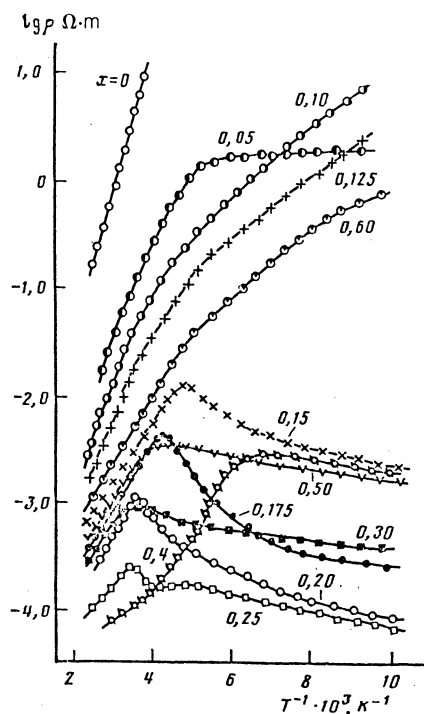


FIG. 8. Temperature dependences of the electric resistance of the solid solutions $\text{La}_{1-x}\text{Ca}_x\text{MnO}_3$.

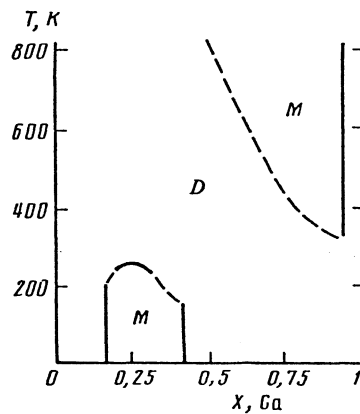


FIG. 9. Change in the electric properties in the system $\text{La}_{1-x}\text{Ca}_x\text{MnO}_3$: M —temperature and Ca-density ranges where the electric conductivity decreases with increasing temperature, as in the case of metals; D —temperature and Ca-density ranges where the electric conductivity increases with increasing temperature, as in the case of semiconductors.

tions we determined the boundaries of the T - x regions (Fig. 8 and Fig. 9).

The basic features of the transition in the interval $0.15 < x < 0.4$ are the following.

1. The resistivity at $T = 4.2$ K ranges from 1 to 10^{-3} $\Omega \cdot \text{cm}$. The values 10^{-3} $\Omega \cdot \text{cm}$ were obtained only for single crystals.²²

2. Electric conductivity remains above the transition temperature, as in the case of semiconductors, with activation energy 0.06–0.14 eV, right up to temperatures of the order of 1000 K. As the temperature decreased to 4.2 K the sample with $x = 0.3$ did not revert to semiconductor conductivity.

3. The transition to activated conductivity usually coincides with the ferromagnet-paramagnet transition, but this may not occur at the periphery of the T - x region.

4. We did not observe a jump in the electric conductivity at the transition. A jump was likewise not observed for single crystals.²² However Japanese investigators observed a jump in the electric conductivity by a factor of three in investigations of a very high-quality ceramic sample, prepared by the coprecipitation method.²³

5. Attempts to measure the Hall effect in a wide range of temperatures and Ca concentrations were unsuccessful, possibly because of the low carrier mobility. The thermo-emf is positive, and at the transition into the high-temperature phase it increases sharply and gradually decreases with increasing temperature. In Ref. 23 a jump in the thermo-emf was observed.

It is extremely difficult to analyze the experimental data because of the large number of crystal-structural and magnetic phase transformations. However we can give a number of well-substantiated conclusions.

The conductivity $10^2 < \sigma < 10^3$ $\Omega^{-1} \cdot \text{cm}^{-1}$ is too low for normal metals. These values are close to the minimum metallic conductivity for $3d$ oxides.²⁴ The low charge-carrier mobility indicates a narrow conduction band.

The compounds $\text{La}_{1-x}^{3+}\text{Ca}_x^{2+}\text{Mn}^{3+}\text{O}_{3-x/2}$ are dielectrics whose crystal-structural parameters and magnetic-phase transformation temperatures are close to those of the system in which the manganese ions have a mixed valence.¹¹ For this reason, in the latter system conductivity should appear

in the impurity band, most likely formed by impurity centers of the type $\text{Ca}^{2+} + \text{Mn}^{4+}$. The strong electron-phonon interaction narrows the band. According to Mott,²⁴ a concentration transition to metallic conductivity in doped systems occurs when two Hubbard bands, formed by the states $\text{Ca}^{2+} + \text{Mn}^{4+}$ and $\text{Ca} + 2\text{Mn}^{4+}$, start to overlap, and the conduction band should be wide enough so that Anderson localization of charge carriers could not occur. For perovskites the transition usually occurs at $x \approx 0.2$. Such a transition was investigated in detail in $\text{La}_{1-x}\text{Ca}_x\text{VO}_3$.²⁵ However the impurity band is narrower in manganites than in vanadites. This is because the zone is formed by e_g orbitals and not t_{2g} orbitals, as in chromites and vanadites. Another important difference in the insulator-metal transition in manganites is that the metallic phase is ferromagnetic, while in other perovskites it is antiferromagnetic or paramagnetic. According to Ref. 23, above T_c local magnetic order remains in manganites right up to temperatures of $\sim 2.5T_c$. We believe that at T_c magnetic disorder results in localization of states near the Fermi energy. This should be accompanied by a very small jump in the conductivity. Using the Mott-Anderson terminology,²⁴ the high-temperature phase in the proposed phase is a Fermi glass.

3.7. Exchange interactions

We believe that the transition to ferromagnetic ordering cannot be governed by indirect exchange interaction via the carriers. This assertion is supported by the following facts.

1. The transition temperature T_c is approximately the same in the insulators $\text{La}_{1-x}\text{Ca}_x\text{MnO}_{3-x/2}$ and conducting perovskites $\text{La}_{1-x}\text{Ca}_x\text{MnO}_3$.¹¹

2. The phase diagram of the system $\text{La}_{1-x}\text{Ca}_x\text{MnO}_3$ is substantially different from the diagram calculated on the basis of the "double exchange" model.⁵

3. The transition to metallic conductivity in other systems of complicated oxides with perovskite structure is not accompanied by the appearance of ferromagnetism.

It should be noted that in many systems of doped oxides and chalcogenides the effect of charge carriers on the change in the Curie temperature is not obvious. In EuO it proved possible to increase T_c from 68 to 160 K without changing the electric conductivity.²⁶ The magnetic properties of $\text{La}_{1-x}\text{Sr}_x\text{CoO}_3$ and CuCr_2Se_4 can be understood without appealing to the theory of double exchange.²⁷

It follows from phase diagrams of manganites (Figs. 3 and 7) that the magnetic two-phase nature is closely associated with the crystal structure. The ferromagnetic phase is only O -orthorhombic, while the orbital and electronic ordering result in antiferromagnetism.

In the orbitally disordered phase the ferromagnetic part of the exchange will be determined by electronic excitations from the half-filled e_g orbital of the Mn^{3+} ion into an unoc-

cupied orbital and is proportional to¹²

$$J \sim b^2 V / U^2,$$

where b is the electron transfer integral, V is the intra-atomic energy splitting of states with different spin, and U is the energy necessary for placing an electron into an unoccupied orbital.

The antiferromagnetic part is determined by transitions between half-filled orbitals and is proportional to¹²

$$J \sim b^2 / (U + V).$$

In the case of a relatively wide $3d$ band (small values of U) the ferromagnetic part of the exchange can predominate. Large values of the cubic cell parameter and the angle Mn-O-Mn (criteria for ferromagnetism, according to Watanabe¹³ and Havinga¹⁴) correspond to this case. Goodenough proposed that correlations in the filling of orbitals of neighboring ions should enhance ferromagnetic exchange. Our IR-spectroscopic data for manganites are consistent with this hypothesis.

¹G. H. Jonker, *Physica* **22**, 707 (1956).

²J. Tanaka, K. Takanashi *et al.*, *Phys. Status Solidi A* **80**, 621 (1983).

³T. M. Perekalina, B. Ya. Kotyuzhanskii, and A. Ya. Shapiro, *Fiz. Tverd. Tela* **32**, 1242 (1990) [*Sov. Phys. Solid State* **32**(4), 731 (1990)].

⁴C. Zener, *Phys. Rev.* **82**, 403 (1951).

⁵P. G. de Gennes, *Phys. Rev.* **118**, 141 (1960).

⁶E. O. Wollan and W. C. Koehler, *Phys. Rev.* **118**, 141 (1960).

⁷Z. Jirak, S. Vratislav *et al.*, *Phys. Status Solidi A* **52**, K39 (1979).

⁸A. T. Starovoitov, V. I. Ozhogin, and V. A. Bokov, *Fiz. Tverd. Tela* **11**, 2153 (1969) [*Sov. Phys. Solid State* **11**(8), 1780 (1970)].

⁹E. L. Nagaev, *Magnetic Materials with Complicated Exchange Interactions* [in Russian], Nauka, Moscow (1989).

¹⁰V. A. Bokov, N. A. Grigorijan *et al.*, *Phys. Status Solidi* **28**, 835 (1968).

¹¹I. O. Troyanchuk, L. V. Balyko, and G. L. Bychkov, *Fiz. Tverd. Tela* **31**, 292 (1989) [*Sov. Phys. Solid State* **31**(4), 716 (1989)].

¹²J. B. Goodenough, *Magnetism and the Chemical Bond*, Interscience, New York (1963).

¹³H. Watanabe, *J. Phys. Soc. Jpn.* **16**, 433 (1961).

¹⁴E. E. Havinga, *Phillips Res. Rep.* **21**, 432 (1966).

¹⁵A. K. Bogush, V. I. Pavlov, and L. V. Balyko, *Crystal Res. Technol.* **18**, 589 (1983).

¹⁶V. E. Wood, A. E. Austin *et al.*, *J. Phys. Chem. Sol.* **34**, 859 (1973).

¹⁷V. J. Pavlov, G. L. Bychkov, and A. K. Bogukh, *Cryst. Res. Technol.* **21**, 487 (1986).

¹⁸S. Querel-Ambrunaz, *Bull. Soc. Fr. et Crystallogr.* **91**, 339 (1968).

¹⁹K. I. Kugel' and D. I. Khomskii, *Usp. Fiz. Nauk* **130**, 621 (1980) [*sic*].

²⁰Rao G. V. Subba and C. N. R. Rao, *Appl. Spectrosc.* **24**, 436 (1970).

²¹E. Pollert, S. Krupicka, and E. Kuzmicova, *J. Phys. Chem.* **43**, 1137 (1982).

²²K. P. Belov, E. P. Svirina, and O. E. Portugal, *Fiz. Tverd. Tela* **20**, 3492 (1978) [*Sov. Phys. Solid State* **20**(11), 2021 (1978)].

²³J. Tanaka, M. Umehara *et al.*, *J. Phys. Soc. Jpn.* **51**, 1236 (1982).

²⁴N. Mott, *Metal-Insulator Transitions*, Taylor and Francis, London (1974).

²⁵M. Sayer, R. Chen, V. Fletcher *et al.*, *J. Phys. C* **8**, 2059 (1975).

²⁶A. S. Borukhovich, V. G. Bamburov, M. S. Morunya *et al.*, *Zh. Eksp. Teor. Fiz.* **72**, 1439 (1977) [*Sov. Phys. JETP* **45**(4), 755 (1977)].

²⁷E. Methfessel and D. Mattis, *Magnetic Semiconductors*, in *Handb.d.J. Physik*, Springer, Vol. 18, p. 389 (1968).

Translated by M. E. Alferieff